ADVANCED ENGINEERING MATERIALS
www.aem-journal.com

An Insight into Machining of Thermally Stable Bulk Nanocrystalline Metals

Vincent H. Hammond, Thomas L. Luckenbaugh, Michael Aniska, David M. Gray, Joshua A. Smeltzer, B. Chad Hornbuckle, Christopher J. Marvel, Kiran N. Solanki, Tony Schmitz, and Kristopher A. Darling*

Recent advances have enabled the production of nano-grained metallic alloys with a thermally stable microstructure. Consequently, the production of bulk samples and subsequent machining and testing of standardized test specimens is now a real possibility. Therefore, for the first time, the authors report on the in-depth characterization and machinability of bulk nanocrystalline materials. In particular, this study addresses the feasibility of machining and to what extent, if any, the microstructure is altered due to the high stresses and temperature incurred during machining. Toward that goal, a series of copper–tantalum nanocrystalline threaded cylindrical tensile samples are machined from extruded rods. Advanced characterization techniques, such as transmission electron microscopy, are employed which indicated that the grain size of the Cu–Ta alloy was further reduced by approximately one-third. This reduction in grain size is quite noteworthy given an estimated total strain of 260% and moderate temperature increase resulting from the machining operation. This unexpected grain refinement is attributed to tantalum-based nanoclusters dispersed through the matrix which limit grain growth in the initial microstructure during machining. Overall, the authors observe a continuous chip formation and machinability of bulk nanocrystalline materials, which stems from stable nano-grains and having a near elastically perfectly plastic material behavior.

1. Introduction

Machining is a controlled material removal process in which a material is shaped by using a defined cutting edge to remove material in the form of thin chips. During such cutting processes, a large shear strain is induced by the tool-material interaction as the chip is formed. Because of its localized nature, the rate of deformation and subsequent heat generation can be quite high. For instance, deformation rates during machining are on the order of $10^3\,s^{-1}$ or higher and approximately 98% of the energy dissipated by metal deformation is manifested as heat or thermal energy that results in a significant increase in temperature, oftentimes on the order of several hundred degrees.[1–3] This extreme condition localized near and at the tool–chip interface (high temperature, pressure, and intense friction) can result in significant changes in the material microstructure. For example, conventional machining has been used as a viable technique to make materials with nano-grained microstructure.[4–9] However, the very same process of producing nano-grained materials, that is, by machining, has never been used to study the machinability of bulk nano-grained materials (materials containing crystallite sizes <100 nm). This is in part due to the inability to process stable nano-grained materials at the bulk scale. However, recent efforts on kinetically stabilized nano-grained materials[10–16] are allowing researchers to produce bulk specimens of complex geometries suitable for full-scale

Dr. V. H. Hammond, D. M. Gray, Dr. B. C. Hornbuckle, Dr. K. A. Darling
Weapons and Materials Research Directorate
US Army Research Laboratory
6300 Rodman Road
Aberdeen Proving Ground, MD 21005
E-mail: vincent.h.hammond.civ@mail.mil

T. L. Luckenbaugh
Bowhead Total Enterprise Solutions, LLC
Belcamp, MD 21017

M. Aniska
Oak Ridge Institute for Science and Education Program
US Army Research Laboratory
Aberdeen Proving Ground, MD 21005

J. A. Smeltzer, Dr. C. J. Marvel
Department of Materials Science and Engineering
Lehigh University
Bethlehem, PA 18015

Prof. K. N. Solanki
School for Engineering of Matter, Transport, and Energy
Arizona State University
Tempe, AZ 85287

Prof. T. Schmitz
Department of Mechanical Engineering and Engineering Science
University of North Carolina – Charlotte
Charlotte, NC 28223

DOI: 10.1002/adem.201800405

 © 2018 WILEY-VCH Verlag GmbH & Co. KGaA, Weinheim

experiments for the very first time. Therefore, in order to truly capture the promise of these materials in actual components, a detailed understanding is required in how these nanocrystalline materials respond to conventional machining operations. Such aspects cannot be overlooked with regards to nanocrystalline metals, as the high stresses, strain rates, and elevated temperatures associated with machining are expected to dramatically alter their initial microstructure.

Therefore, here we report for the first time general observations of machining and its effect on the stabilized grain structure in nanocrystalline metals. In particular, we examine machining induced strain localization and its role on continuous chip formation as well as surface finish. For this purpose, a series of optimized nanocrystalline copper–tantalum (Cu–3 at% Ta) rods (average grain size of 86 nm) manufactured through powder metallurgy were machined to produce ASTM E8/E8M-08 standard cylindrical threaded specimens suitable for large scale testing. Advanced microstructural characterization techniques, such as scanning electron microscopy (SEM), were used to probe the chip morphology and post-machining characterization of the final surface. Similarly, scanning transmission electron microscopy (S(TEM)) was utilized to characterize the extent to which machining altered the microstructure within the chips. Such aspects are critical and yield important information on the cutting process. The results reveal that stabilized nanocrystalline microstructures undergo significant grain-refinement. This finding is atypical of traditional nanocrystalline metals which are prone to undergo grain growth due to elevated temperature and/or deformation. Further, formation of long continuous chips along with excellent surface finish suggest a very low cutting force relative to the yield stress of ~1 GPa and, potentially, low tool wear. This excellent machinability in a stable nanocrystalline material stems from stable nano-grains and having a near elastically perfectly plastic material behavior along with high elastic stiffness (low harmful vibrations).[10] These collected aspects are captured with high-speed (1000 fps) digital photography, showing that bulk nanocrystalline metals formed by powder consolidation can be effectively machined for intended purposes. Overall, the ability to make and machine ASTM conventional mechanical testing samples not only opens the door to new fundamental studies, but also demonstrates the next step in viable commercialization of bulk structural components, something which has lagged behind other niche nonstructural applications for many years.

2. Experimental Section

A series of stabilized Cu–3 at% Ta (hereafter designated as Cu–3Ta) rods were produced from mechanically alloyed powders. The mechanically alloyed powder was placed within a Ni billet. The billet containing the powder is heated to 700 °C and then sent through a multi-pass equal channel angular extrusion (ECAE) process to consolidate the powder. After this process, the consolidated powder had experienced a total strain of 460%. Complete details of the powder processing and consolidation efforts can be found in ref. [16]. Microstructural analysis of the rods using TEM (**Figure 1**a–c) indicates that the extruded microstructure for this alloy was found to have an average grain size of 84.4 nm. Prior statistical analysis revealed the presence of an extremely dense network of Ta-based nanoclusters with a mean diameter of 2 nm within the microstructure.[10,13,17] These nanoclusters are observed to exist within the Cu matrix and along grain boundaries, as shown in Figure 1b. It has been previously determined that such nanoclusters play an important role in dictating the mechanical response as well as stabilizing the matrix grain size under the application of stress and temperature such as during processing and mechanical testing.[10–12,14,16] The rods of stabilized nanocrystalline Cu–3Ta were machined into threaded cylindrical tensile samples using standard machining practices. Machining chips from the stabilized Cu-3Ta rods were collected and subsequently examined in order to identify microstructural changes using an FEI Nova600i Nanolab dual beam focused ion beam (FIB)/SEM. (S)TEM analysis was performed using a JEOL 2100F operating at 200 kV on TEM lift-outs from selected regions of the turnings.

3. Results and Discussion

The progression of an ECAE processed rod to final machined test specimen is shown in **Figure 2**. A core (approximately 10 mm in diameter) containing the consolidated Cu–3Ta powder was machined from the center of the rectangular nickel billet along the long axis using electric discharge machining (EDM). A live-center was created at the tip of the Cu–3Ta rod to reduce wobble during turning operations. The remnants of the Ni can were removed by turning on a Haas ST10 CNC lathe using a Sandvik CNMG 12 04 08-PM 4325 cutting insert with a cutting speed of 84 cms^{-1} (2000 rpm), a feed of 0.08 mm per revolution at a cutting depth of 0.130 mm per pass to reveal the consolidated Cu–3Ta rod, as seen in Figure 2a and **Movie 1**. The finished rod of Cu–3Ta was approximately 5–6 cm in length and 6.35 mm in diameter. A remaining portion of the Ni can was used as a base for the lathe chuck to grip during machining. To produce the ¼-28 UNF 1A thread, the turned down cylinder was then threaded on the same lathe over its entire length (Figure 2b) using a Carmex 11 ER AGO BMA single-point, external threading insert operating at a cutting speed of 120 cms^{-1} (3000 rpm) and a feed of 0.94 mm per revolution with a 60° lead-in angle (**Figure 3**a and **Movie 2**). In general, the rods were easily threaded with minimal irregularities present in the threads (Figure 3b). Figure 3c and Movie 2 illustrate two important points with regards to machining bulk nanocrystalline Cu–3Ta. First, the machining chips are continuous and secondly, harmful vibrations are minimal. This behavior is significant because it indicates a low rate of tool wear. The gauge lengths were then cut, again on the same lathe, using a Sandvik N123G2-0300-0004-TM 1125 flat-edge parting tool insert with a cutting speed of 150 cms^{-1} (3600 rpm), a feed of 0.18 mm per revolution, and a cutting depth of 0.05 mm per pass (Figure 2c). The machined sample was then put on a small manual lathe where the gauge lengths were polished using strips of silicon carbide sandpaper with grits ranging from 320 to 1200. The gauge lengths were then polished to a 1 μm finish using a diamond slurry and the samples separated by wire EDM by cutting to the desired length ~5 cm (Figure 2c,d). This process was repeated several times to produce multiple tensile samples (Figure 3d) and tensile fatigue

© 2018 WILEY-VCH Verlag GmbH & Co. KGaA, Weinheim

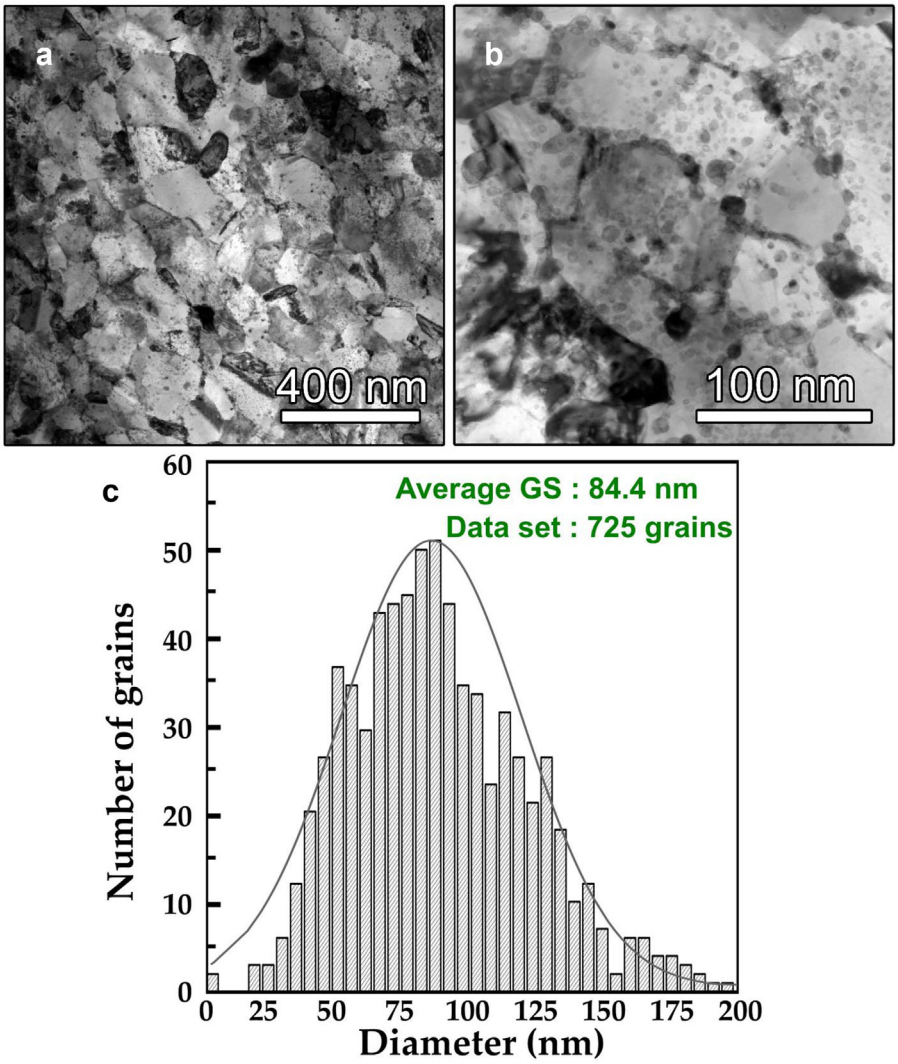

Figure 1. a) Low magnification (scanning) transmission electron microscopy (S)TEM Bright Field (BF) image of as-received (i.e., post-ECAE processed) sample showing grain structure. b) High magnification STEM BF TEM image showing the high density of Ta-based clusters residing in the lattice as well as along the grain boundaries of the Cu-based matrix. c) Grain size distribution plot of the ECAE processed sample.

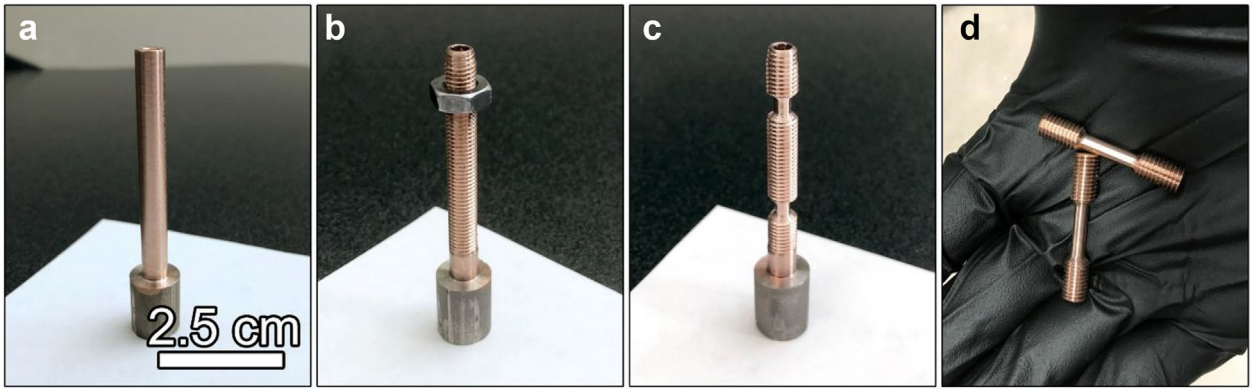

Figure 2. Progression of an ECAE processed rod to final test specimen by machining. a) A core produced via EDM. b) Turned down and threaded core. c) Initial cutting of two distinct gauge sections for two independent cylindrical tensile samples. d) Final tensile samples approximately 38.1 mm in length.

 © 2018 WILEY-VCH Verlag GmbH & Co. KGaA, Weinheim

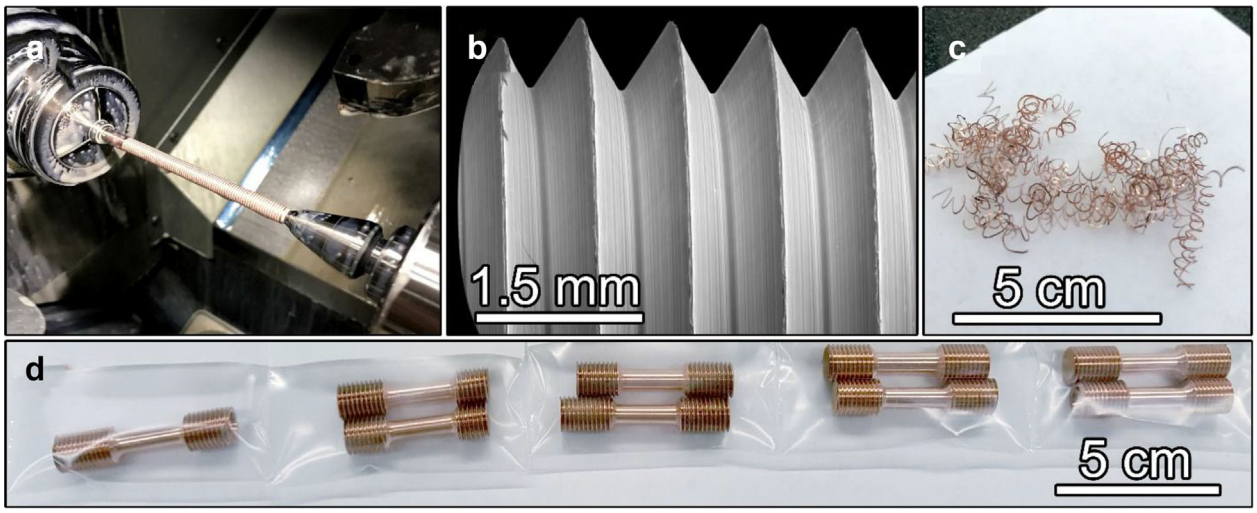

Figure 3. Threading process. a) Image of the core still in the lathe after being turned and threaded to the appropriate dimensions. b) SEM image showing the respective surface finish of individual threads. c) Representative turning from the machining process. d) Numerous tensile samples showing uniformity and reproducibility of the machining process for Cu–3Ta.

samples (Supplemental Figure S1). This documentation of the successful machining of ASTM standard samples represents a significant step forward in realizing the fabrication and commercialization of structural parts made of stabilized bulk nanocrystalline metals.

Differences in surface appearance resulting from the lathe rather than EDM cutting are shown in **Figure 4**. In contrast to the relatively smooth surface left by the lathe (left side in Figure 4a, b), the EDM surface is rougher and shows evidence of melting that occurred due to the intense heat generated during the EDM process (Figure 4c). Finally, the surface of the machined sample does not show any cracking perpendicular to the cutting surface or material pullout resulting from the machining process (Figure 4d). However, some small depressions were observed which could be related to crack formation ahead of the cutting tool, galling, and/or other localized events. Capturing such events is outside the scope of this work and will be relayed in a later publication. Examination of the chips obtained during the machining operation indicated that many of them are continuous pieces 50–70 mm in length that are shiny in appearance (Figure 3c and 5) and uniform in thickness. Higher magnification imaging in an SEM (**Figure 6**) reveals the interior surface (b) sliding against the tooling is relatively smooth. While viewing from the exterior surface (c), the machining chip appears pleated

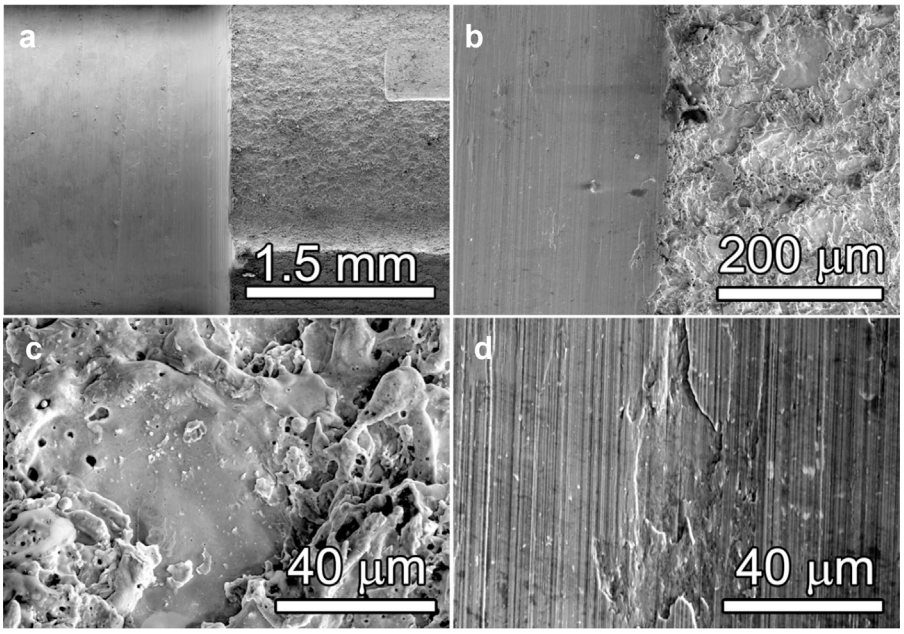

Figure 4. Difference in surface appearance resulting from the lathing and EDM cutting. a, b) Low and medium magnification SEM images of the lathed surface (left side) and EDM surface (right side). c, d) High magnification SEM images of the EDM surface c) and the lathed surface d).

 © 2018 WILEY-VCH Verlag GmbH & Co. KGaA, Weinheim

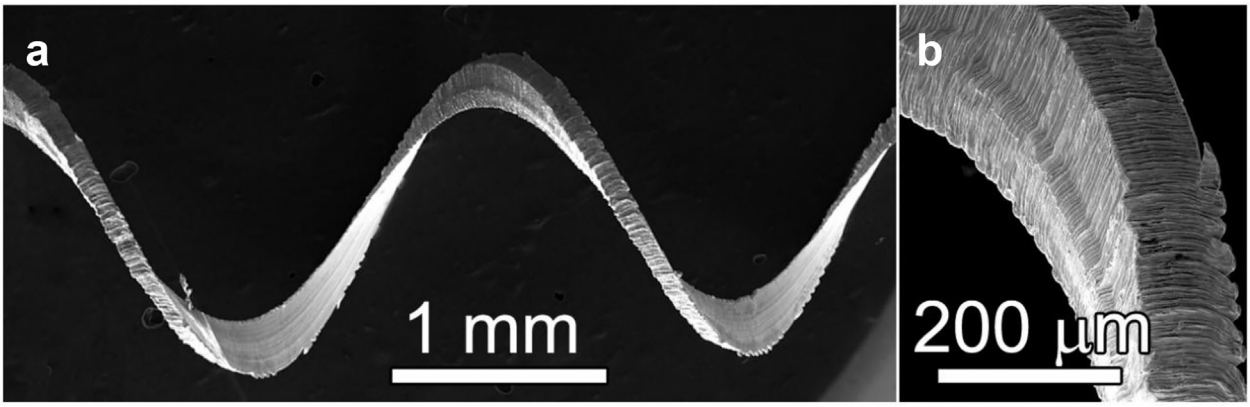

Figure 5. a) Low magnification SEM image showing the spiral of an individual turning. b) Medium magnification SEM image showing the morphology of the backside of a turning.

because of the intense shear plane of deformation and its oscillation during continuous chip formation. Viewing from the side (d) reveals the appearance of incremental shear or localization events which protrude only partially though the thickness of the turning. This serrated chip profile is typically the result of the competition between strain hardening and thermal softening as the chip is formed. Overall, these observations indicate excellent machinability.

The images in **Figure 7**a–c focus on the pleated surfaces seen in Figure 6c and of the stabilized Cu–3Ta alloy. Shown in Figure 7a, b is the exterior pleated machining surface induced during turning. As reported earlier, the starting grain size for the Cu–3Ta alloy is approximately 84 nm. The remaining image, Figure 7c, is a higher magnification SEM image showing a dimple structure on the surface of the machining chip. If these dimple structures are indeed the grains of the alloy, then the average size appears to be much finer than the starting average grain size. To prove the extent of grain refinement as a result of machining, (S)TEM was utilized for microstructural characterization. The fractured end of a chip is shown in **Figure 8**a. A TEM lift out from the chip surface (Figure 8b) with statistical analysis (Figure 8c) reveals that the average grain size is approximately

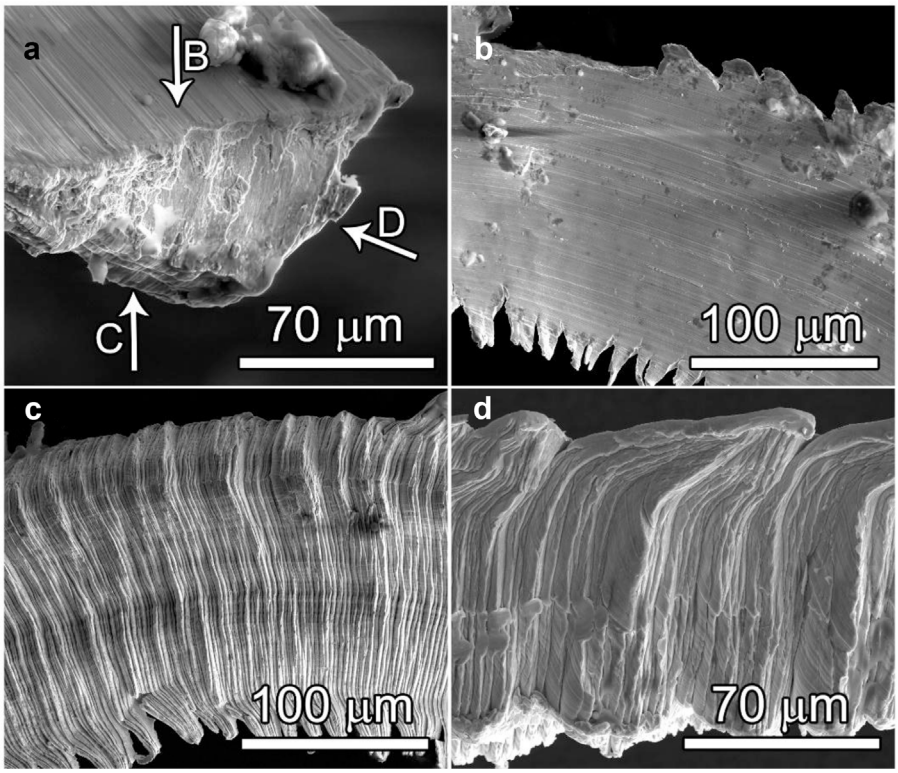

Figure 6. a) High magnification SEM images of the machine turnings. b) Interior surface sliding against the tool (side B). c) Viewing from (side C). d) Viewing from (side D).

 © 2018 WILEY-VCH Verlag GmbH & Co. KGaA, Weinheim

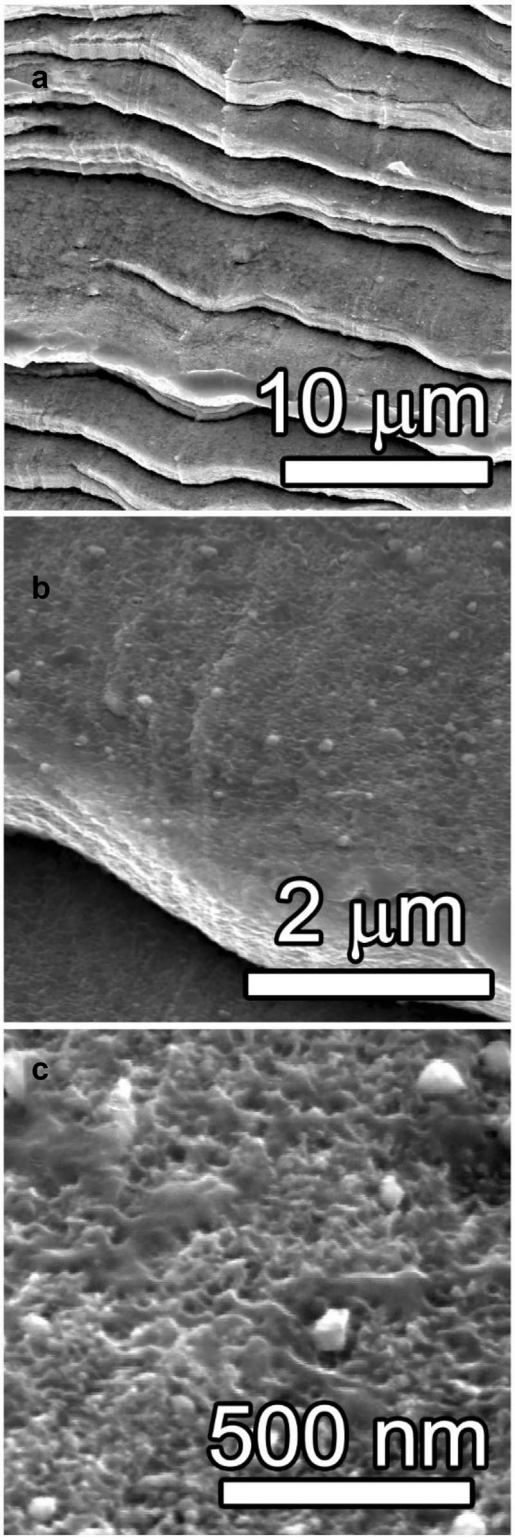

Figure 7. a, b, c) SEM micrographs of progressively increased magnification showing the pleated surface of a machining chip from stabilized nanocrystalline Cu–3Ta.

30 nm, which is approximately one-third that of the starting grain size. This was found to be true in the orthogonal direction as well. Topological analysis using SEM indicates that the fracture surface in Figure 8a consists of ductile dimples approximately 100 nm (Supplemental Figure S2) in size with some regions across the fracture surface being much larger (approximately several hundred nm). Thus, multiple grains are involved in the deformation process leading to failure, indicative of a ductile material.

Machining is considered a severe plastic deformation process; that is, the raw material is subjected to a high amount of dynamic shear compressive stress and strain combined with moderately high temperature rises (typically 200–400 °C).[1–3] Thus, the mixed mechanical and thermal loading applied during the machining process can lead to extensive grain refinement in coarse grain materials through dynamic recrystallization. In fact, a large body of literature exists that is primarily focused on the production of nanocrystalline chips from these types of machining operations.[4–9] However, applying this same rationale to the machining of bulk nanocrystalline metals may not hold true as thermomechanical loading is generally known to induce rapid grain growth. For instance, deformation-induced grain growth in nanocrystalline materials is a widely reported phenomenon that has been observed during uniaxial tension testing,[18–20] fatigue,[21] and testing under cryogenic temperatures.[22] A similar behavior is observed during various severe plastic deformation processes such as high pressure torsion and high-energy ball milling where a tenfold increase in initial grain size was reported.[5,11,12] Specifically, with nanocrystalline Cu, Zhang et al.[22] reported rapid grain coarsening from 20 nm to about 200–300 nm as a result of indentation testing.

Unlike the aforementioned un-stabilized nanocrystalline metals, nanocrystalline Cu–3Ta alloys have a dense network of Ta-based clusters dispersed though the matrix. The growth kinetics of these clusters for all practical purposes is temperature independent and the mean size and spatial distribution remain constant regardless of temperature and deformation.[13,17] Based on the Zener pinning effects, these particles dispersed throughout the matrix provided a potent mechanism for stabilizing grain size. In turn, the accrued thermomechanical energy as a result of machining can be harnessed for further grain refinement in such systems as stabilized nanocrystalline Cu–3Ta. In fact, in situ high magnification imaging at the tip of an orthogonal cutting tool, as described in ref. [23] revealed the primary shear plane angle during cutting of nanocrystalline Cu–3Ta to be approximately $24.5 \pm 1°$. Utilizing the parallel plate model, it can be estimated that the active shear strain endured by the sample is approximately 260%. The equation governing the parallel plate model is $\gamma = \tan(\phi - \alpha) + \cot\phi$, where γ = shear strain, ϕ = shear plane angle, and α = rake angle of cutting tool. The localized dynamic nature of the deformation and the magnitude of shear strain in the case reported can result in deformation-induced shear bands and regions of high dislocation densities within the matrix. Even with the occurrence of a local temperature rise, the heavily deformed microstructure underwent grain refinement due to the machining process rather than grain growth typically seen when nanocrystalline materials experience deformation and/or a temperature increase. Overall, we present a first systematic study on machinability of thermally stable nanocrystalline materials, which is important for a detailed

© 2018 WILEY-VCH Verlag GmbH & Co. KGaA, Weinheim

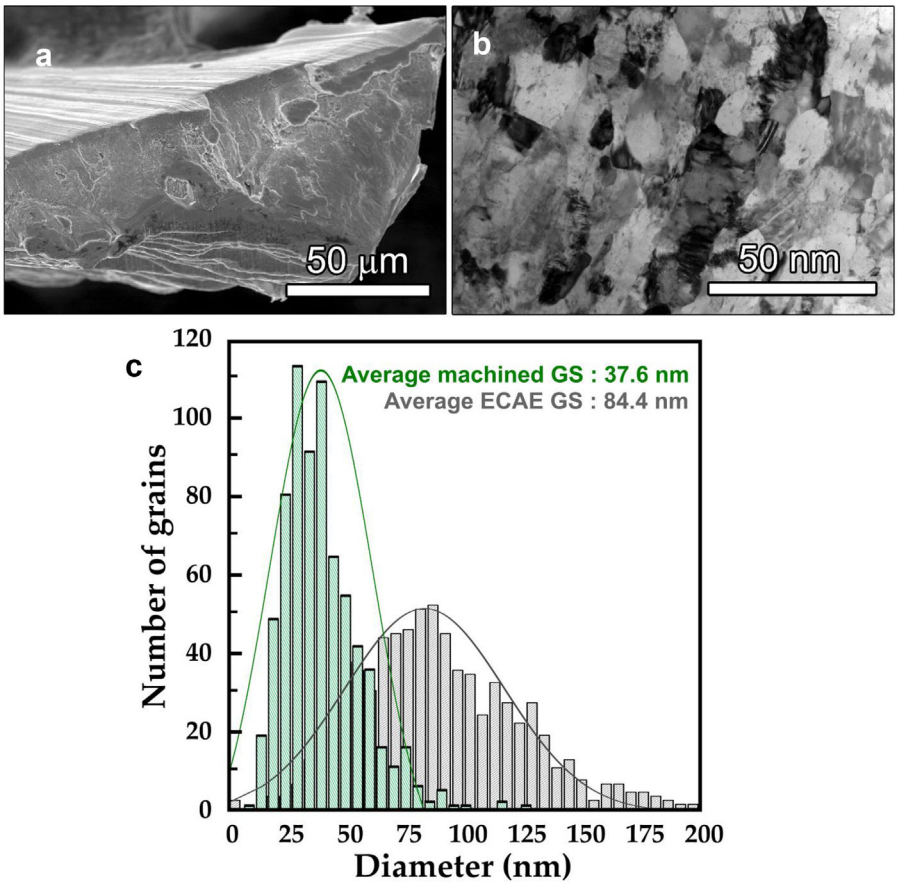

Figure 8. a) SEM image showing the fractured end of a typical turning. b) (S)TEM BF image showing the average grain size within the chip to be 30 nm. c) Grain size distribution plot for Cu–3Ta after being ECAE processed and machined, respectively.

understanding of the chip formation and tool wear mechanism in such materials and found that homogeneous deformation of working material with near elastic-plastic response yields continuous chip formation and excellent surface finish.

4. Conclusions

A series of threaded cylindrical test specimens have been machined from Cu–3Ta rods produced from mechanically alloyed powders using an ECAE processing protocol. Although several studies have detailed the high coarsening resistance of these alloys to elevated temperatures, this was the first effort to determine the response of this material to the temperatures and stresses induced by machining operations. The result reveals that the grain size was reduced approximately threefold due to the strain induced during machining. This behavior is in noted contrast to the general observation of rapid microstructural coarsening in conventional nanocrystalline metals under similar conditions. This difference in behavior is attributed to the presence of Ta clusters throughout the Cu–3Ta alloy, which acted to restrict grain growth during the machining process where high rate stresses and local temperature rises occur. Further, examination of the chips obtained during the machining operation indicated that many of them are continuous pieces 50–70 mm in length that are shiny in appearance and uniform in thickness. Thus, formation of long continuous chip along with excellent surface finish at relatively high cutting speeds suggest a very low cutting force and, potentially, low tool wear. This excellent machinability in a stable nanocrystalline material stems from stable nano-grains and having a near elastically-perfectly plastic material behavior along with high elastic stiffness (low harmful vibrations).

Acknowledgements

K.N.S. acknowledges the support of the US Army Research Laboratory under contract W911NF-15-2-0038 and a National Science Foundation grant number 1663287.

Supporting Information

Supporting information is available online from the Wiley Online Library or from the author.

Conflict of Interest

The authors declare no conflict of interest.

 © 2018 WILEY-VCH Verlag GmbH & Co. KGaA, Weinheim

Keywords

grain refinement, machinability, nanocrystalline, thermal stability

Received: April 19, 2018
Revised: July 26, 2018
Published online:

[1] E. M. Trent, P. K. Wright, *Metal Cutting*, Fourth ed., Butterworth Heinemann, Boston, MA **2000**.
[2] J. Tlusty, *Manufacturing Processes and Equipment*, Prentice Hall, Upper Saddle River, NJ **2000**.
[3] S. Kalpakjian, S. Schmid, *Manufacturing Processes for Engineering Materials*, Fifth ed., Prentice Hall, Upper Saddle River, NJ **2008**.
[4] M. R. Shankar, S. Chandrasekar, A. H. King, W. D. Compton, *Acta Mater.* **2005**, *53*, 4781.
[5] Y. Idell, G. Facco, A. Kulovits, M. R. Shankar, J. M. K. Wiezorek, *Scr. Mater.* **2013**, *68*, 667.
[6] F. Ambrosy, F. Zanger, V. Schulze, *CIRP Annals* **2015**, *64*, 69.
[7] F. Ambrosy, F. Zanger, V. Schulze, I. S. Jawahir, *Procedia CIRP* **2014**, *13*, 169.
[8] P. Iglesias, M. D. Bermudez, W. Moscoso, B. C. Rao, M. R. Shankar, S. Chandrasekar, *Wear* **2007**, *263*, 636.
[9] S. Akcan, W. S. Shah, S. P. Moylan, S. Chandrasekar, P. N. Chhabra, H. T. Y. Yang, *Metall. Mater. Trans. A* **2002**, *33*, 1245.
[10] K. A. Darling, C. Kale, S. Turnage, B. C. Hornbuckle, T. L. Luckenbaugh, S. Grendahl, K. N. Solanki, *Scr. Mater.* **2017**, *141*, 36.
[11] K. A. Darling, M. Rajagopalan, M. Komarasamy, M. A. Bhatia, B. C. Hornbuckle, R. S. Mishra, K. N. Solanki, *Nature* **2016**, *537*, 378.
[12] K. A. Darling, E. L. Huskins, B. E. Schuster, Q. Wei, L. J. Kecskes, *Mat. Sci. Eng. A* **2015**, *638*, 322.
[13] T. Rojhirunsakool, K. A. Darling, M. A. Tschopp, G. P. P. Pun, Y. Mishin, R. Banerjee, L. J. Kecskes, *MRS Commun.* **2015**, *5*, 333.
[14] M. Rajagopalan, K. A. Darling, S. Turnage, R. K. Koju, B. C. Hornbuckle, Y. Mishin, K. N. Solanki, *Mater. Des.* **2017**, *113*, 178.
[15] K. A. Darling, A. J. Roberts, Y. Mishin, S. N. Mathaudhu, L. J. Kecskes, *J. Alloy Compd.* **2013**, *573*, 142.
[16] K. A. Darling, M. A. Tschopp, R. K. Guduru, W. H. Yin, Q. Wei, L. J. Kecskes, *Acta Mater.* **2014**, *76*, 168.
[17] B. C. Hornbuckle, T. Rojhirunsakool, M. Rajagopalan, T. Alam, G. P. P. Pun, R. Banerjee, K. A. Darling, *JOM* **2015**, *67*, 2802.
[18] G. J. Fan, L. F. Fu, H. Choo, P. K. Liaw, N. D. Browning, *Acta Mater.* **2006**, *54*, 4781.
[19] J. A. Sharon, P. C. Su, F. B. Prinz, K. J. Hemker, *Scr. Mater.* **2011**, *64*, 25.
[20] D. S. Gianola, S. Van Petegem, M. Legros, S. Brandstetter, H. Van Swygenhoven, K. J. Hemker, *Acta Mater.* **2006**, *54*, 2253.
[21] H. A. Padilla, B. L. Boyce, *Exp. Mech.* **2010**, *50*, 5.
[22] K. Zhang, J. R. Weertman, J. A. Eastman, *Appl. Phys. Let.* **2005**, *87*, 061924.
[23] Y. Guo, W. D. Compton, S. Chandrasekar, *Proc. R. Soc. A* **2015**, *471*, 20150194.

 © 2018 WILEY-VCH Verlag GmbH & Co. KGaA, Weinheim